

Trigeminal neuralgia associated with a solitary pontine lesion: clinical and neuroimaging definition of a new syndrome

Sarasa Tohyama^{a,b}, Peter Shih-Ping Hung^{a,b}, Joshua C. Cheng^c, Jia Y. Zhang^a, Aisha Halawani^{a,d}, David J. Mikulis^{b,d}, Jiwon Oh^e, Mojgan Hodaie^{a,b,f,g,*}

Abstract

Conventional magnetic resonance imaging of patients with trigeminal neuralgia (TN) does not typically reveal associated brain lesions. Here, we identify a unique group of TN patients who present with a single brainstem lesion, who do not fulfill diagnostic criteria for multiple sclerosis (MS). We aim to define this new clinical syndrome, which we term TN associated with solitary pontine lesion (SPL-TN), using a clinical and neuroimaging approach. We identified 24 cases of SPL-TN, 18 of which had clinical follow-up for assessment of treatment response. Lesion mapping was performed to determine the exact location of the lesions and site of maximum overlap across patients. Diffusion tensor imaging was used to assess the white-matter microstructural properties of the lesions. Diffusivity metrics were extracted from the (1) SPL-TN lesions, (2) contralateral, unaffected side, (3) MS brainstem plaques from 17 patients with TN secondary to MS, (4) and healthy controls. We found that 17/18 patients were nonresponders to surgical treatment. The lesions were uniformly located along the affected trigeminal pontine pathway, where the site of maximum overlap across patients was in the area of the trigeminal nucleus. The lesions demonstrated abnormal white-matter microstructure, characterized by lower fractional anisotropy, and higher mean, radial, and axial diffusivities compared with the unaffected side. The brainstem trigeminal fiber microstructure within a lesion highlighted the difference between SPL-TN lesions and MS plaques. In conclusion, SPL-TN patients have identical clinical features to TN but have a single pontine lesion not in keeping with MS and are refractory to surgical management.

Keywords: Trigeminal neuralgia, Lesion, Multiple sclerosis, Lesion mapping, Diffusion tensor imaging, Tractography

1. Introduction

Trigeminal neuralgia (TN) is the most common type of chronic neuropathic facial pain,²⁶ characterized by intermittent attacks of severe, electric shock-like unilateral pain along the distribution of the trigeminal nerve branches.¹³ It has been described as one of the most excruciating pains a human can suffer,⁴⁸ causing

significant distress and deterioration in quality of life.⁴⁷ Although not essential to TN pathophysiology, a well-established etiological factor is neurovascular compression of the trigeminal nerve at the root entry zone,^{2,32,35} where focal demyelination is believed to occur at the point of contact.^{10,30} Trigeminal neuralgia can also manifest secondary to multiple sclerosis (MS-TN),³³ where demyelinating brainstem plaques are believed to be responsible for the paroxysmal, lancinating pain.³⁰

Advances in neuroimaging techniques have identified key neuroanatomical signatures that distinguish TN. Diffusion tensor imaging (DTI) studies have shown white-matter microstructural abnormalities at the trigeminal root entry zone characterized by lower fractional anisotropy (FA),^{8,19,28,31} and higher mean diffusivity (MD), radial diffusivity (RD), and axial diffusivity (AD).⁸ These metrics derived from DTI have been associated with pathophysiological mechanisms: FA is highly sensitive to overall white-matter microstructural changes, while MD, RD, and AD can provide a specific assessment of neuroinflammation,¹ myelination,^{42,44} and axonal integrity,⁴³ respectively. In addition, multi-tensor DTI tractography has revealed differences in brainstem trigeminal fiber microstructure between patients with TN and MS-TN.⁷

Towards our goal to further understand TN, we applied these advanced neuroimaging techniques to study a new, unique group of patients with TN who present with an unusual condition, namely a single brainstem lesion. Magnetic resonance imaging (MRI) of these patients does not identify any other brain lesions or atrophy, and patients do not fulfill criteria for the diagnosis of

Sponsorships or competing interests that may be relevant to content are disclosed at the end of this article.

^a Division of Brain, Imaging, and Behaviour, Systems Neuroscience, Krembil Research Institute, Toronto Western Hospital, University Health Network, Toronto, ON, Canada, ^b Institute of Medical Science, Faculty of Medicine, University of Toronto, Toronto, ON, Canada, ^c Stony Brook University School of Medicine, Stony Brook, NY, United States, ^d Division of Neuroradiology, Joint Department of Medical Imaging, Toronto Western Hospital, University Health Network, Toronto, ON, Canada, ^e Division of Neurology, Department of Medicine, St. Michael's Hospital, Toronto, ON, Canada, ^f Department of Surgery, Faculty of Medicine, University of Toronto, Toronto, ON, Canada, ^g Division of Neurosurgery, Krembil Neuroscience Centre, Toronto Western Hospital, University Health Network, Toronto, ON, Canada

*Corresponding author. Address: Division Neurosurgery, Toronto Western Hospital, 399 Bathurst St, 4W W-443, Toronto, ON M5T 2S8, Canada. Tel.: (416) 603-6441; fax: (416) 603-5298. E-mail address: mojgan.hodaie@uhn.ca (M. Hodaie).

PAIN 161 (2020) 916–925

Copyright © 2019 The Author(s). Published by Wolters Kluwer Health, Inc. on behalf of the International Association for the Study of Pain. This is an open access article distributed under the terms of the Creative Commons Attribution-Non Commercial-No Derivatives License 4.0 (CCBY-NC-ND), where it is permissible to download and share the work provided it is properly cited. The work cannot be changed in any way or used commercially without permission from the journal.

<http://dx.doi.org/10.1097/j.pain.0000000000001777>

multiple sclerosis (MS). The lesions seem to be distributed along the trigeminal nerve pathway; however, the exact location of the lesions with respect to the trigeminal nucleus is unknown. The lesions also appear to be consistent with demyelination, but conventional MRI demonstrates their significant differences from MS plaques, in that they appear much more distinct. On top of this, from a clinical perspective, these patients seem to respond poorly to surgical treatment. Although single cases or very small case series of TN patients with brainstem lesions exist in the literature,^{3,6,23,24,34,38} this unique entity has not been defined as a syndrome and studied extensively.

Thus, the aim of this study was to define a new clinical syndrome, which we term TN associated with solitary pontine lesion (SPL-TN), using a clinical and neuroimaging approach. Towards this aim, we hypothesized that (1) there is a cohort of patients with TN that will exhibit a single brainstem lesion and no other supratentorial or infratentorial lesions. We also hypothesized that (2) these patients will be nonresponders to surgical treatment, (3) the lesions will be distributed along the affected trigeminal brainstem pathway based on lesion mapping, and (4) the microstructural properties of the lesions will be significantly different from MS plaques and healthy controls based on DTI metrics and tractography.

2. Materials and methods

2.1. Definition of clinical population: trigeminal neuralgia associated with solitary pontine lesion

We defined SPL-TN based on the following criteria: (1) diagnosis of idiopathic TN according to the third edition of the International Classification of Headache Disorders (ICHD-3)¹⁸ and (2) presence of a single brainstem lesion along the trigeminal nerve pathway and no other supratentorial or infratentorial lesions. According to the new ICHD-3,¹⁸ these patients fall under the diagnostic criteria of idiopathic TN because they have clinical features consistent with TN but either do not have neurovascular contact or have neurovascular contact without evidence of morphological changes (eg, atrophy or displacement) in the trigeminal nerve root demonstrated on MRI. Patients with SPL-TN do not have TN secondary to MS, cranial tumors, or vertebral basilar dolichoectasia brainstem compression.

We retrospectively reviewed the MRI and clinical records of 481 patients who underwent neurosurgical treatment for TN at the Toronto Western Hospital in Canada between June 2004 and May 2018. Details of the surgical treatments performed, including Gamma Knife radiosurgery, microvascular decompression surgery, and percutaneous trigeminal rhizotomy have been previously described by our group.^{20,46} The lesions were identifiable on a T1-weighted anatomical MR image. The study was approved by the University Health Network Research Ethics Board. Healthy control participants were recruited from the community and provided written informed consent according to the Declaration of Helsinki before the study. The inclusion criteria for the healthy controls were (1) no previous history of neurologic, psychiatric, or pain conditions, (2) no major surgery of the central nervous system, and (3) no contraindications for MRI.

Clinical assessment, including a screening neurological examination and focused examination of the cranial nerves, was performed for each patient on their first clinical visit to the neurosurgery center by an experienced neurosurgeon (M.H.). All patients had clinical symptoms consistent with TN, purely paroxysmal, according to the ICHD-3,¹⁸ characterized by recurrent, severe, electric shock-like attacks of unilateral pain

along the distribution of the trigeminal nerve branches, triggered by innocuous stimuli such as wind, chewing, touching the face, and brushing the teeth. There were no clinical sensory abnormalities detectable, such as paresthesia and/or numbness of the affected trigeminal nerve branches. Patients had no previous clinical history or events suggestive of MS and were seen by multiple teams of physicians, including neurologists, neuro-radiologists, and neurosurgeons, none of whom indicated the possibility of MS and confirmed the diagnosis of TN. Clinical examination did not suggest any other facial pain disorder.

To further confirm that patients with SPL-TN do not fulfill criteria for the diagnosis of MS, 2 neuroradiologists (A.H. and D.J.M.) with MS-related expertise independently reviewed the MRI and clinical records of the patients identified. The diagnosis of MS was excluded, on both clinical and radiological grounds, according to the latest 2017 McDonald criteria.⁴⁵ Therefore, overall, the clinical symptomatology of these patients was indistinguishable from classical or idiopathic TN. However, they presented with a single brainstem lesion unrelated to MS.

2.2. Assessment of treatment response

To assess treatment response, all SPL-TN patients with clinical follow-up data for at least 6 months were included. The outcome measure was pain intensity as measured by an 11-point Numerical Rating Scale (NRS) (0-10: no pain–worst possible pain) and the Barrow Neurological Institute (BNI) scale (I: no trigeminal pain, no medication; II: occasional pain, no medication; III: some pain, adequately controlled with medication; IV: some pain, not adequately controlled with medication; V: severe pain, no pain relief). Because we hypothesized SPL-TN patients to be a specific group of nonresponders, we determined nonresponders as (1) having undergone multiple, repeat interventions (ie, ≥ 3 surgical procedures) or (2) having undergone one surgical procedure with inadequate pain relief (ie, $< 75\%$ reduction in preoperative pain and a BNI score of IV or V), and the decision to not have further surgery for the time being. The 75% cutoff and BNI scores I to III have both been previously used to determine effective surgical treatment for TN.^{9,25,46}

2.3. Neuroimaging acquisition

As part of our routine clinical imaging protocol, each patient underwent MRI (3T GE) sessions with an 8-channel phased-array head coil to acquire T1-weighted FSPGR anatomical scans (voxel size = $0.94 \times 0.94 \times 1 \text{ mm}^3$, matrix = 256×256 , repetition time = 12 ms, echo time = 5.1 ms, inversion time = 300 ms, flip angle = 20° , field of view = 24 cm), T1-weighted FLAIR scans (voxel size = $0.43 \times 0.43 \times 3 \text{ mm}^3$, matrix = 512×512 , repetition time = 2367 ms, echo time = 13 ms, inversion time = 860 ms, echo train length = 6, flip angle = 90°), and T2-weighted FIESTA scans (voxel size = $0.39 \times 0.39 \times 0.80 \text{ mm}^3$, matrix = 512×512 , repetition time = 4.5 ms, echo time = 2.2 ms, flip angle = 37°). For a subset of patients, diffusion-weighted imaging scans (60 directions, spin echo EPI sequence, $1 B_0$, $b = 1000 \text{ s/mm}^2$, 1 excitation, ASSET, voxel size = $0.94 \times 0.94 \times 3 \text{ mm}^3$, matrix = 256×256 , repetition time = 12,000 ms, echo time = 86.4 ms, flip angle = 90° , field of view = 24 cm) were also acquired. Each healthy control participant underwent an MRI session using the same scanner, to acquire a T1-weighted FSPGR anatomical scan and a diffusion-weighted imaging scan with the same parameters as described above.

Given the nature of the patient group being refractory to surgical management, a subset of patients was referred to our

neurosurgical center having already undergone previous surgical procedure(s). This created a limitation in our ability to study pre-treatment imaging data in all patients. Thus, we used the earliest imaging time point available for our analyses. A total of 14 SPL-TN patients had T1-weighted imaging before treatment, all of whom exhibited a single brainstem lesion before undergoing their first surgery. To further ensure that the lesion is not an effect of the treatment given, we compared the volume (mm^3) and location of the lesions in a subset of 7 SPL-TN patients who had imaging before and after treatment (mean post-treatment time point \pm SD: 6.93 ± 2.10 months). For each patient, the lesion was mapped by hand in T1 space at both the pre- and post-treatment time points using 3D Slicer v4.3.1.¹⁴ The change in lesion volume (mm^3) before and after treatment was calculated for each patient using the percentage change formula. Mean differences in lesion volume were evaluated using the Wilcoxon signed-rank test. To compare the location of the lesion before and after treatment, each patient's pre-treatment T1 image was linearly registered to their post-treatment T1 image using FLIRT in FSL v5.0.²² The lesion mask in post-treatment T1 space was then overlaid onto the pre-treatment T1 image to see whether the lesion before treatment was contained within the voxels of the mask drawn after treatment.

2.4. Evaluation of neurovascular contact

T2-weighted FIESTA images were evaluated to determine the proportion of SPL-TN patients that had neurovascular contact on the symptomatic and/or asymptomatic side of the trigeminal nerve(s). Patients were excluded from this evaluation if they had undergone a microvascular decompression surgery before referral to our center.

2.5. Lesion mapping

Brain lesions were mapped by hand in T1 space using 3D Slicer. The remaining steps were performed in FSL. Nonbrain tissues were removed using the Brain Extraction Tool (BET) within FEAT, followed by nonlinear registration to standard MNI152-2 mm space using FNIRT. The resulting subject lesion maps were binarized and added together using fsmaths to determine the distribution of lesions and area with the highest overlap across subjects.

2.6. Diffusion-weighted imaging processing

Diffusion-weighted images were eddy current and motion corrected in FSL, followed by diffusion tensor estimation and derivation of scalar maps (ie, FA, MD, RD, and AD) using 3D Slicer. Each subject's T1-weighted anatomical image was then linearly registered to their diffusion tensor image, highlighting alignment of the midpontine region of the brainstem where the lesions are located. To align each SPL-TN patient to their matched healthy control, nonlinear registration was performed using Advanced Normalization Tools (ANTs).⁴

2.7. Microstructural analysis

Microstructural analysis was performed in a subset of SPL-TN patients who had diffusion-weighted imaging scans. Diffusivity metrics (FA, MD, RD, and AD) were extracted from 3 region of interest (ROI) locations using 3D Slicer: (1) the lesion ROI was defined as the single brainstem lesion; (2) the unaffected ROI was defined as the contralateral spatially equivalent control region of the brainstem; and (3) the control ROI was defined as the region

identical to the lesion ROI and unaffected ROI (ie, left and right sides of the brainstem), averaged in an age-/sex-matched healthy control.

2.8. Microstructural comparison of solitary pontine lesions and multiple sclerosis plaques

2.8.1. Patients with trigeminal neuralgia secondary to multiple sclerosis

To compare the microstructural properties of the brainstem lesions between SPL-TN and MS-TN patients, surgically naïve MS-TN patients with brainstem plaques along the trigeminal nerve pathway were included through retrospective review of MRI and clinical records. The same clinical imaging protocol and diffusion-weighted imaging processing pipeline was used as describe above. Diffusivity metrics (FA, MD, RD, and AD) were extracted using a whole-lesion and tract-restricted approach.

2.8.2. Whole-lesion approach

The MS plaque ROI was defined as all brainstem plaques along the trigeminal nerve pathway on the affected side. For patients with multiple plaques, diffusivity measurements were averaged across all ROIs. Metrics from this ROI were compared with those derived from the lesion ROI of SPL-TN patients.

2.8.3. Tract-restricted approach

To assess microstructural changes specific to the brainstem trigeminal fibers within a lesion, the trigeminal nerve tracts for each SPL-TN and MS-TN patient were reconstructed using eXtended Streamline Tractography.⁴⁰ eXtended Streamline Tractography is a multitensor deterministic DTI tractography technique that can trace through neural areas that have dense crossing fibres, such as the brainstem. We have previously shown successful visualization of the brainstem trigeminal fibers using this technique in patients with MS-TN.⁷ Specifically, ROIs were placed bilaterally at the trigeminal root entry zone in each patient's diffusion tensor image, and XST was performed using the following parameters: Westin planar threshold = 0.2, tensor fraction = 0.2, radius of curvature = 0.8 mm, minimum length = 10 mm, and step size = 1 mm. Once the brainstem trigeminal fibers were successfully reconstructed, the lesion ROI in SPL-TN patients and MS plaque ROI in MS-TN patients were restricted to only the voxels where the trigeminal nerve brainstem tracts were present.

2.9. Statistical analysis

Average differences within groups were evaluated using paired-samples *t*-tests or Wilcoxon signed-rank tests where appropriate. Average differences between groups were evaluated using independent-samples *t*-tests or Mann-Whitney *U* tests where appropriate. A one-way analysis of covariance was conducted to compare the differences in diffusivity metrics between SPL-TN and MS-TN patients while controlling for age and pain duration at MRI date. The proportion of sex in each patient group was assessed using the χ^2 test. All statistical analyses were computed in SPSS v 22.0 (IBM, Armonk, NY). Multiple comparisons were corrected for all 4 diffusivity metrics for each separate analysis using false discovery rate correction. Statistical significance was determined at $P < 0.05$ or q (false discovery rate-corrected P -value) < 0.05 when adjustments were necessary for multiple comparisons.

3. Results

3.1. Clinical groups

We found 24 cases of SPL-TN (15 men and 9 women, mean age \pm SD: 70.2 \pm 10.7 years), 18 of which had sufficient clinical follow-up data for assessment of treatment response. We excluded one patient for being the only responder, leaving a total of 17 SPL-TN patients (12 men and 5 women, mean age \pm SD: 70.4 \pm 11.3 years) in our lesion mapping analyses. Of these, 11 had diffusion-weighted imaging scans for microstructural analysis of the lesions. Thus, 11 SPL-TN patients (7 men and 4 women, mean age \pm SD: 66.4 \pm 10.2 years) and 11 age-/sex-matched healthy controls (7 men and 4 women, mean age \pm SD: 64.6 \pm 10.0 years) were included in our DTI analyses. There was no significant difference in age between patients and controls ($t_{(20)} = 0.40, P = 0.69$).

The analysis performed to ensure that the lesion is not an effect of the treatment given showed no statistically significant change in T1 lesion volume (mm³) before and after treatment ($Z = -0.68, P = 0.50$). The mean percentage change in lesion volume \pm SD was 0.14% \pm 0.0086. The lesion location also remained the same as the lesion present before treatment was contained within the voxels of the mask drawn after treatment. Neurovascular contact of the trigeminal nerve was less common in this population and were equally present on the symptomatic (8/18, 44%) and asymptomatic side (8/18, 44%). There were no instances of neurovascular contact causing distortion or atrophy of the trigeminal nerve.

We further identified 17 MS-TN patients (6 men and 11 women, mean age \pm SD: 52.1 \pm 10.0 years) for comparison of brainstem lesions between SPL-TN and MS-TN patients. The 2 groups were matched for age of onset of TN (mean age of TN onset \pm SD_{SPL-TN} = 52.2 \pm 11.7 years, mean age of TN onset \pm SD_{MS-TN} = 47.4 \pm 8.91 years; $t_{(23)} = 1.17, P = 0.30$). The number of MS brainstem plaques along the affected trigeminal nerve pathway varied across MS-TN patients (mean number \pm SD: 1.76 \pm 1.15, range 1-5 plaques). Compared with MS-TN patients, SPL-TN patients were significantly older ($t_{(26)} = 3.67, P = 0.0011$) and had longer duration of TN on MRI date (mean number of years \pm SD_{SPL-TN} = 13.9 \pm 9.07, mean number of years \pm SD_{MS-TN} = 5.00 \pm 4.52; $t_{(12,01)} = 2.87, P = 0.014$).

The distribution of sex between the SPL-TN and MS-TN group was not significantly different ($\chi^2(1) = 2.16, P = 0.14$). See **Figure 1** for a flow chart of patient selection and MR images of a sample of SPL-TN and MS-TN patients.

3.2. Patients with trigeminal neuralgia associated with solitary pontine lesion are nonresponders to surgical treatment

Seventeen of 18 patients with SPL-TN were nonresponders to surgical treatment, unrelated to the type of surgery they underwent. Patients had frequent recurrence of pain and repeated procedures (mean number of surgeries \pm SD: 4.11 \pm 2.42, range: 1-9). Of these 17 nonresponders, 14 underwent 3 or more surgical procedures. The 3 patients who underwent one surgical procedure had a 0%, 0%, and 37.5% reduction in preoperative pain and BNI scores of V, V, and IV, respectively, at their last follow-up. The single responder achieved a 100% reduction in preoperative pain and BNI score I from Gamma Knife radiosurgery treatment at the last, 8-year follow-up. The mean follow-up period for all patients was 57.9 months (range: 6.0-157.3 months). Details of these patients are provided in **Table 1**.

3.3. Lesion mapping reveals the distribution of solitary pontine lesions

In all 17 cases, the location of the lesion was in the pons along the affected trigeminal nerve pathway (**Fig. 2**). Six patients had right-sided lesions, and 11 patients had left-sided lesions. The site of maximum overlap (9/11 patients with left-sided lesions) was in the area of the trigeminal brainstem sensory nuclear complex (VBSNC).

3.4. Solitary pontine lesions demonstrate abnormal white matter microstructure

SPL-TN lesions showed significantly lower FA ($t_{(10)} = -5.08, P = 4.8 \times 10^{-4}, q = 7.4 \times 10^{-4}$), and higher MD ($t_{(10)} = 4.98, P = 5.5 \times 10^{-4}, q = 7.4 \times 10^{-4}$), RD ($t_{(10)} = 5.61, P = 2.3 \times 10^{-4}$),

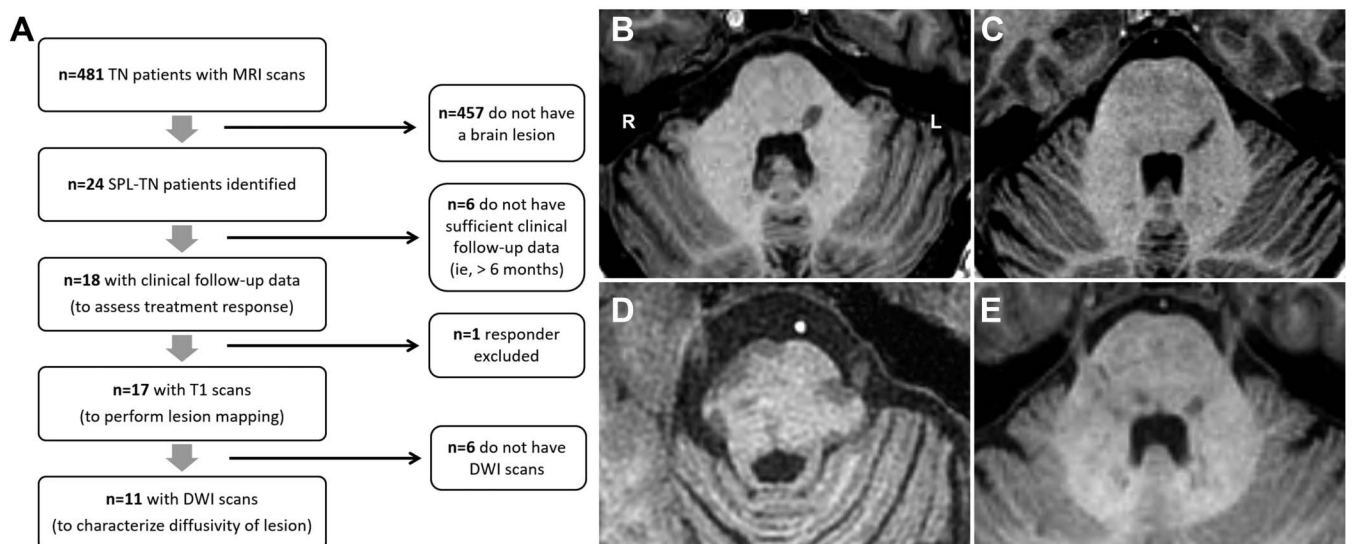


Figure 1. Flow chart of patient selection and MR images of a sample of SPL-TN and MS-TN patients. (A) Flow chart of SPL-TN patient selection and experimental design. (B–E) Axial T1-weighted anatomical images of the midpontine region of the brainstem in a sample of patients. (B and C) The single, distinct pontine lesion in 2 different SPL-TN patients (both left-sided pain). (D and E) The multiple, diffuse MS brainstem plaques in 2 different MS-TN patients (left- and right-sided pain, respectively). MR, magnetic resonance; MS, multiple sclerosis; SPL-TN, TN associated with solitary pontine lesion; TN, trigeminal neuralgia.

Table 1

SPL-TN patient demographic and clinical characteristics.

ID	Sex	Age (y)	TN onset age (y)	Pain side	Pain distribution	TN duration (y)	Pain med(s)	Type of surgery	No. of surgeries	Scans
01	F	43	31	L	V1/2/3	12	BCF, CZM, HYD	GK, MVD, PTR	5	T1, DWI
02	F	69	48	R	V2/3	21	GBP, OXC, PHT	GK, MVD, PTR	4	T1, DWI
03	F	82	51	L	V2/3	31	CBZ, OXY, PGB	GK, MVD, PN, PTR	9	T1, DWI
04	M	70	45	L	V2/3	25	CBZ	GK, PTR	5	T1, DWI
05	M	65	61	L	V3	4	CBZ	GK	1	T1, DWI
06	M	72	58	L	V1/2	14	CBZ, PGB	GK, PTR	3	T1, DWI
07*	F	86	61	L	V2/3	25	None	GK	1	T1, DWI
08	M	66	NA	L	V2/3	NA	CBZ	GK	1	T1, DWI
09	M	64	53	R	V1/2/3	11	PGB	GK, MVD, PTR	4	T1, DWI
10	F	76	41	R	V2/3	35	CBZ	GK, PTR	5	T1, DWI
11	M	73	63	L	V3	10	CBZ	GK, PN, PTR	8	T1, DWI
12	M	79	71	R	V3	8	CBZ	GK, PTR	3	T1, DWI
13	M	74	62	R	V1/2/3	12	CBZ, LEV, MOR, NTP, PGB	GK, MVD, PNS, PTR, tractotomy	8	T1
14	M	87	73	L	V2/3	14	CBZ	GK, PTR	5	T1
15	M	50	45	L	V3	5	CBZ, GBP, NTP	GK	1	T1
16	F	73	63	R	V1/2/3	10	CBZ	GK, MVD, PTR	4	T1
17	M	67	36	L	V3	31	GBP, OXC	GK, PTR	4	T1
18	M	86	56	L	V2/3	30	CBZ	GK, MVD	3	T1

Age (in years), TN duration (in years), and pain medication(s) are based on last clinical follow-up.

All patients have TN, purely paroxysmal.

* Single patient classified as responder. All other patients classified as nonresponders.

BCF, baclofen; CBZ, carbamazepine; CZM, clonazepam; DWI, diffusion-weighted imaging scan; GBP, gabapentin; GK, Gamma Knife radiosurgery; HYD, hydromorphone; LEV, levetiracetam; MOR, morphine; MVD, microvascular decompression; NA, information not available; NTP, nortriptyline; OXC, oxcarbazepine; OXY, oxycodone; PGB, pregabalin; PN, peripheral neurectomy; PNS, peripheral nerve stimulation; PTR, percutaneous trigeminal rhizotomy; PHT, phenytoin; SPL-TN, trigeminal neuralgia associated with solitary pontine lesion; T1, T1-weighted anatomical scan; TN, trigeminal neuralgia.

$q = 7.4 \times 10^{-4}$), and AD ($t_{(10)} = 3.02$, $P = 0.013$, $q = 0.013$) compared with the contralateral, unaffected side. Compared with healthy controls, SPL-TN lesions showed significantly lower FA ($t_{(13.62)} = -2.83$, $P = 0.014$, $q = 0.018$), higher MD ($t_{(20)} = 4.66$, $P = 1.5 \times 10^{-4}$, $q = 3.0 \times 10^{-4}$) and RD ($t_{(20)} = 5.39$, $P = 2.8 \times 10^{-5}$, $q = 1.1 \times 10^{-4}$), with no change in AD ($t_{(20)} = 0.74$, $P = 0.47$, $q = 0.47$). The contralateral, unaffected side did not significantly differ from healthy controls for all diffusivity metrics ($q > 0.05$) (Fig. 3).

3.5. Microstructural differences between solitary pontine lesions and multiple sclerosis plaques

3.5.1. Whole-lesion analysis

When the diffusivity metrics were extracted from the whole SPL-TN lesions and MS plaques, there were no statistically significant differences between the 2 entities for FA ($t_{(26)} = -0.30$, $P = 0.77$, $q = 0.77$), MD ($t_{(26)} = 1.85$, $P = 0.076$, $q = 0.15$), RD ($t_{(26)} = 1.91$, $P = 0.068$, $q = 0.15$), and AD ($t_{(26)} = 1.40$, $P = 0.18$, $q = 0.23$) (Fig. 4A–E). The results remained the same after statistically controlling for age and pain duration at MRI date ($q > 0.05$).

3.5.2. Tract-restricted analysis

The brainstem trigeminal fibers were successfully reconstructed in 8 SPL-TN patients (6 men and 2 women, mean age \pm SD: 69.4 \pm 5.8 years) and 15 MS-TN patients (6 men and 9 women, mean age \pm SD: 51.8 \pm 10.6 years). When the ROI was restricted to only the voxels where the trigeminal brainstem tracts were visible

within the SPL-TN lesion or MS plaque, SPL-TN lesions showed significantly lower FA ($t_{(20.86)} = -2.22$, $P = 0.038$, $q = 0.038$), and higher MD ($U = 10$, $P = 0.0013$, $q = 0.0026$), RD ($U = 6$, $P = 4.9 \times 10^{-4}$, $q = 0.0020$), and AD ($U = 18$, $P = 0.0067$, $q = 0.0089$) compared with MS plaques. The results remained the same after statistically controlling for age and pain duration at MRI date ($q < 0.05$). In addition, MS-TN patients showed significant differences between their whole plaques and restricted trigeminal brainstem tracts for FA ($t_{(14)} = -2.99$, $P = 0.0098$, $q = 0.0098$), MD ($t_{(14)} = 4.08$, $P = 0.0011$, $q = 0.0023$), RD ($t_{(14)} = 3.65$, $P = 0.0026$, $q = 0.0035$), and AD ($t_{(14)} = 4.74$, $P = 3.2 \times 10^{-4}$, $q = 0.0013$). Patients with SPL-TN did not show such differences between their whole lesions and restricted trigeminal brainstem tracts for all diffusivity metrics ($q > 0.05$) (Fig. 4F–I).

3.6. Lesion characteristics of the single responder

Although the single SPL-TN responder was excluded from the group-level lesion mapping and DTI analyses, we compared the responder's lesion location and microstructural properties to the nonresponder group findings. In contrast to the lesions located more centrally in nonresponders, where the highest lesion overlap was in the area of the VBSNC, the responder's lesion was located in the periphery at the trigeminal root entry zone. The patient did not have neurovascular contact on both the symptomatic and asymptomatic side. Diffusivity metrics of FA, MD, and RD of the responder's lesion were also outliers (ie, ± 2 SD away from the mean) and closer to the average diffusivity values of the nonresponders' unaffected side and healthy controls.

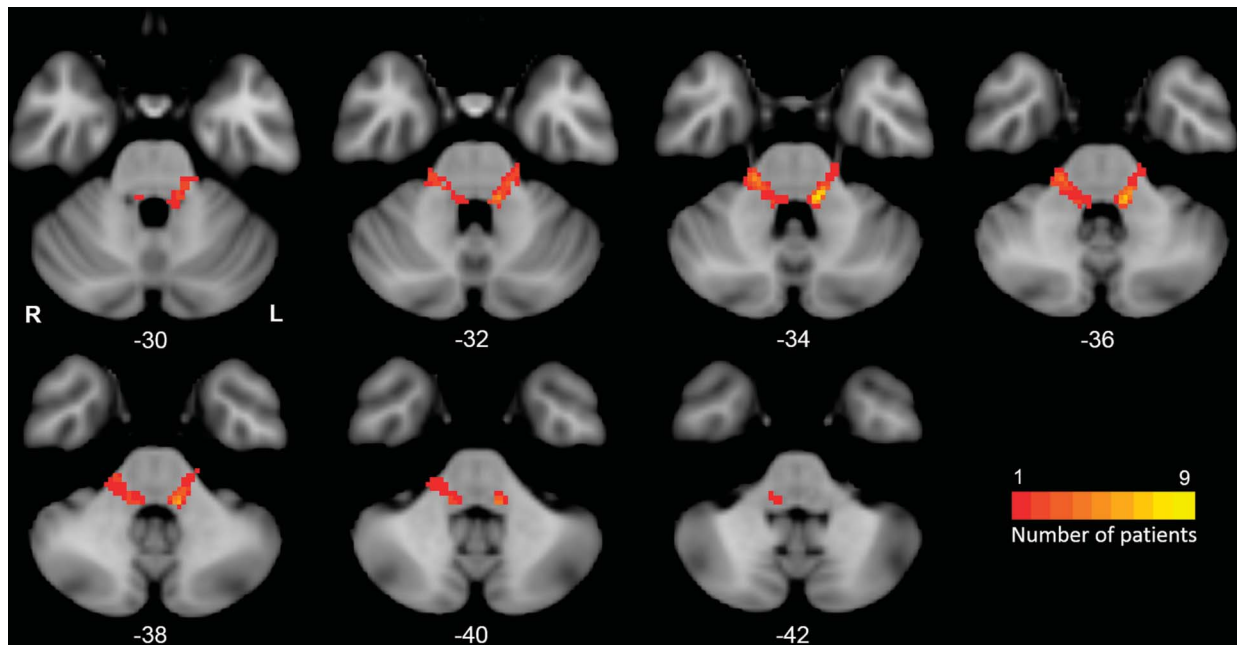


Figure 2. Lesion mapping results in SPL-TN patients. A group-level map of SPL-TN lesions in 17 patients (6 right-sided lesions and 11 left-sided lesions). Maps are overlaid on a T1 template in standard MNI152-2 mm space. MNI coordinates of axial slices (z-axis) are shown. The color scale indicates the number of patients that have a lesion in the given voxel. All lesions are located in the pons along the trigeminal nerve pathway, corresponding to the side of pain. The highest lesion overlap is centered in the area of the VBSNC, peak MNI coordinates (x, y, z): $-10, -38, -34$. SPL-TN, TN associated with solitary pontine lesion; TN, trigeminal neuralgia.

4. Discussion

This study defines the new clinical syndrome of SPL-TN using a clinical and neuroimaging approach. Patients with SPL-TN have clinical features that are identical to TN but have a single pontine lesion not in keeping with MS. The definition of this syndrome and differentiation from other known types of TN are important as these patients are overwhelmingly nonresponders to surgical treatment. The lesions are uniformly distributed along the affected trigeminal pontine pathway, where the greatest lesion overlap across patients is in the area of the VBSNC. Diffusion tensor imaging analyses of the SPL-TN lesions demonstrate abnormal white-matter microstructure, characterized by lower FA, and higher MD, RD, and AD compared with the unaffected side. Furthermore, the brainstem trigeminal fiber microstructure within a lesion, but not the whole lesion itself, highlights the difference between SPL-TN and MS-TN patients. Thus, although conventional MRI cannot directly distinguish MS plaques from SPL-TN lesions, DTI may be capable of anatomically differentiating the 2 when a tract-restricted approach is used. This is important in understanding the potential pathophysiological changes in SPL-TN patients who differ from MS-TN patients.

We find that in our cohort, all but one patient with SPL-TN are nonresponders to surgical treatment, the majority having undergone 3 or more surgical procedures. The high number of surgical procedures, lack of response, and recurrence of pain in this cohort are noteworthy. Typically, neurosurgical procedures for TN are highly effective, with approximately 70 to 80% of patients with classical TN^{11,36,41,49} and 50 to 80% of patients with MS-TN^{12,50,51} achieving long-lasting pain relief after treatment. In cases when patients do not respond or pain recurs, repeat or alternative surgical procedures may be performed. A number of studies have shown that repeat procedures are a feasible option with a good likelihood of success and minimal risk of complications.^{5,17,37} However, it is uncommon for patients to undergo 3 or more procedures. Thus, if we consider treatment response profile as a spectrum across subtypes of TN, our findings suggest that

SPL-TN patients would fall on the extreme end of “nonresponse” and are a critical type of nonresponder. Early identification of these patients is important and points to the role of novel treatment strategies, such as neuromodulation, for their management.

We demonstrate using lesion mapping that SPL-TN lesions are located in the pons along the affected trigeminal nerve pathway, where the highest overlap is in the area of the VBSNC. The VBSNC is involved in processing orofacial somatosensory information, including mechanosensation and nociception. It consists of 2 distinct sensory nuclei—the main trigeminal sensory nucleus and the spinal trigeminal nucleus. The main trigeminal sensory nucleus is the more rostral portion of the VBSNC, located in the dorsal pons. Most fibers related to touch (A β fibers) synapse onto this nucleus, which mediates facial mechanical sensations.²⁹ The spinal trigeminal nucleus is located more caudally and extends along the caudal pons and medulla. A large portion of fibers related to nociception (A δ and C fibres) synapse onto this nucleus, which mediates cranial pain sensation.²⁹ Previous studies have suggested an impairment of inhibitory mechanisms in the spinal trigeminal nucleus may be responsible for the paroxysmal pain in TN.^{16,27} Taken together, our findings provide further evidence for a possible central contribution to TN pain.

To further understand the characteristics of SPL-TN lesions, we used DTI to examine its microstructural properties. We found changes across all diffusivity metrics in the lesions (ie, lower FA, and higher MD, RD, and AD) compared with the contralateral, unaffected side, which suggests overall disruption of white-matter microstructure, as well as specific changes including neuroinflammation,¹ demyelination,^{42,44} and axonal degeneration.⁴³ This was not surprising as T1-weighted anatomical MR images show the lesions to be remarkably distinct. What was unexpected was diffusivity metrics measured from the whole lesion, and not restricted to the trigeminal brainstem tracts, did not demonstrate significant microstructural differences between SPL-TN lesions and MS plaques.

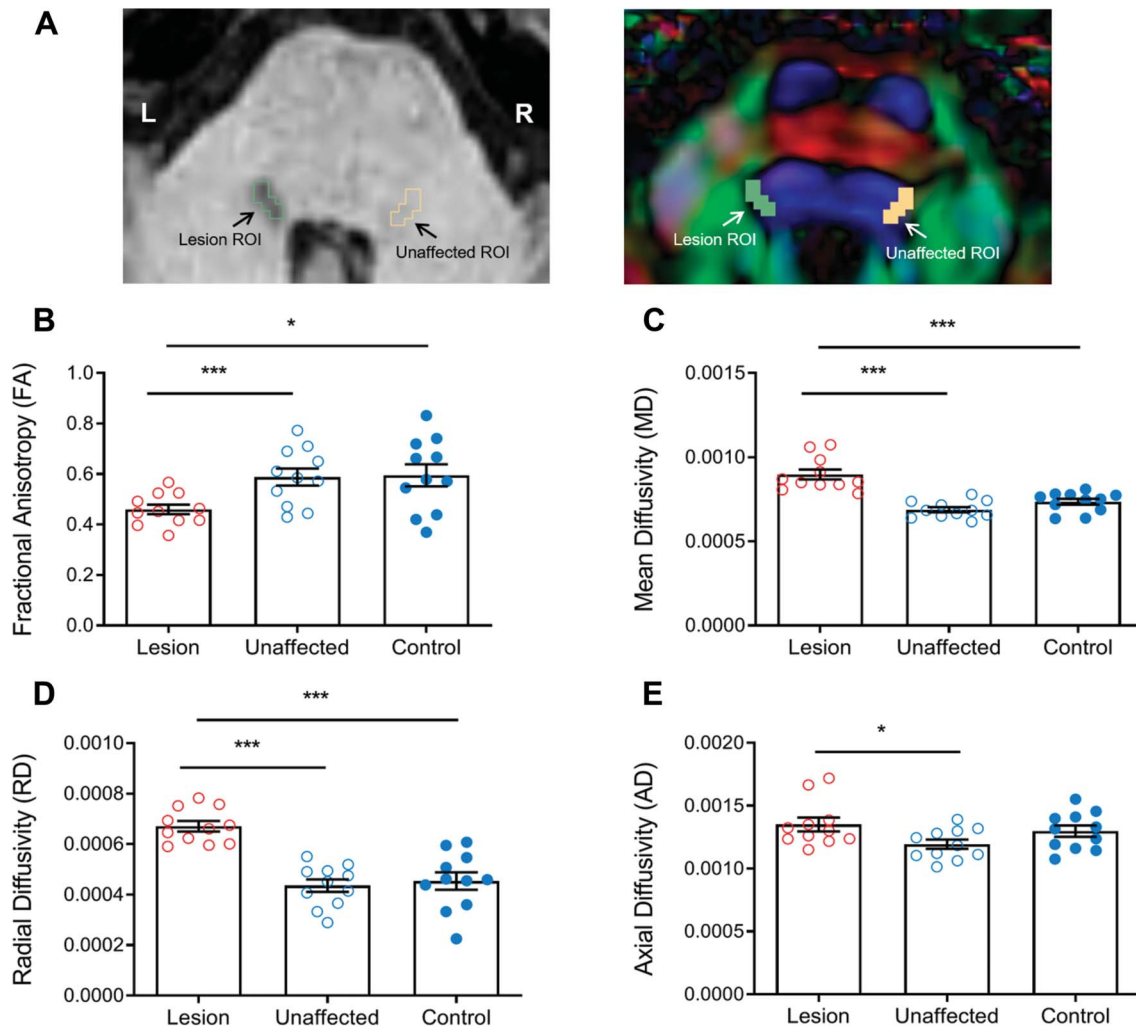


Figure 3. Microstructural properties of SPL-TN lesions. (A) ROI placements for an example SPL-TN patient shown on an axial T1-weighted anatomical image (*left*) and DTI image (*right*). The DTI is shown in color-by-orientation view (red: left-right, green: anterior-posterior, blue: superior-inferior). (B–E) Average microstructural diffusivity metrics (FA, MD, RD, and AD) \pm SEM with overlaid individual data points. Solitary pontine lesions demonstrate characteristically lower FA (B), higher MD (C), RD (D), and AD (E) compared with the contralateral, unaffected side. Except for AD, the same trend remains when compared with healthy controls. * $P < 0.05$, *** $P < 0.001$ (FDR-corrected). AD, axial diffusivity; DTI, diffusion tensor imaging; FA, fractional anisotropy; FDR, false discovery rate; MD, mean diffusivity; RD, radial diffusivity; ROI, region of interest; TN, trigeminal neuralgia.

The pathological hallmark of MS is multiple lesions, or more specifically plaques, within the central nervous system. The dominant pathological feature of MS-related lesions is demyelination, including variable gliosis and inflammation, with relative preservation of axons³⁹—although it is important to note that the histopathology of MS lesions are heterogeneous, as are the number, location, size, and shape of lesions across patients.¹⁵ In MS-TN patients, demyelinating brainstem plaques are believed to be responsible for the paroxysmal, lancinating pain.³⁰ On conventional MRI, MS plaques seem more diffuse and less demarcated compared with SPL-TN lesions. Based on what is known about MS-related lesions, we hypothesized that diffusivity metrics would differ between SPL-TN lesions and MS-TN brainstem plaques. However, we found that DTI did not differentiate between the 2 types of lesions when using a whole-lesion approach.

We examined the brainstem trigeminal fibers of SPL-TN and MS-TN patients using tractography and restricted our diffusivity measurement to only the voxels where the trigeminal brainstem tracts were present within the SPL-TN lesion or MS plaque. This

tract-restricted approach revealed significant differences across all diffusivity metrics (ie, lower FA, and higher MD, RD, and AD) in SPL-TN patients compared with MS-TN patients. Thus, multi-tensor deterministic DTI tractography may objectively distinguish the brainstem trigeminal fiber microstructure of SPL-TN and MS-TN patients. More broadly, our findings suggest that meaningful differences can be masked by extracting diffusivity metrics from the whole lesion because it may include measures unrelated to the tract of interest. This may especially be the case in areas that have dense crossing fibres, such as the brainstem. This points to the importance of considering a tract-restricted approach when performing such an analysis. In addition, our findings provide insight into the specific neuroanatomical features that highlight nonresponse to treatment, where centrally disrupted pontine trigeminal fibers may be a key feature for patients that respond poorly to current surgical treatment modalities. This is consistent with our previous finding in classical TN patients, where nonresponders show presurgical microstructural abnormalities that lie more centrally within the brainstem at the pontine segment.²¹

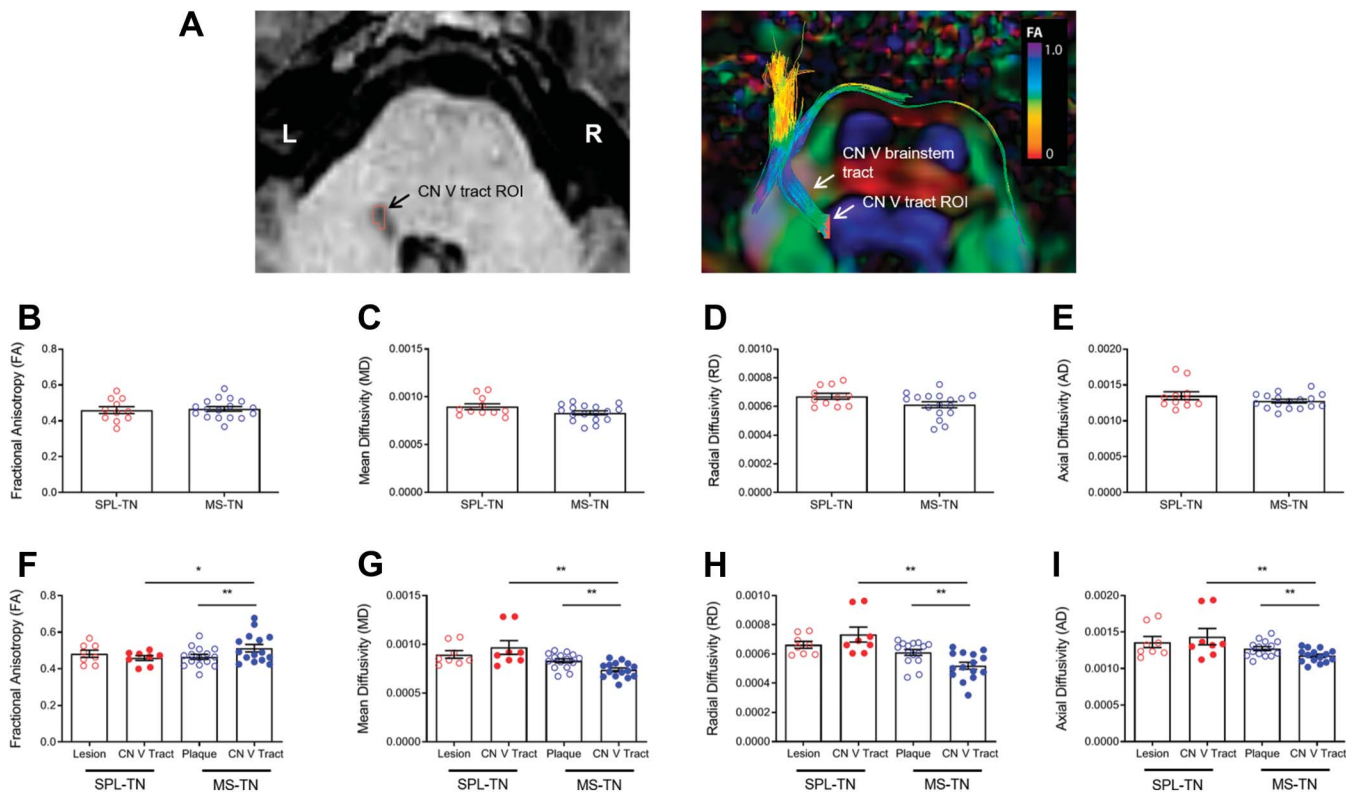


Figure 4. Microstructural differences between SPL-TN lesions and multiple sclerosis plaques. (A) CN V tract ROI placement for an example SPL-TN patient shown on an axial T1-weighted anatomical image (*left*) and DTI image (*right*). The DTI image displays the reconstructed affected trigeminal nerve tracts and successful visualization of the brainstem trigeminal fibers. The color scale indicates the spectrum values of FA (0-1.0) of the tracts. The CN V tract ROI is restricted to only the voxels where the trigeminal brainstem tracts are present within the lesion. (B–I) Average microstructural diffusivity metrics (FA, MD, RD, and AD) ± SEM with overlaid individual data points. The microstructural properties of the whole SPL-TN lesions (red, n = 11) do not differ from MS plaques (blue, n = 17) (B–E). The brainstem trigeminal fibers within a lesion in SPL-TN patients (solid red, n = 8) revealed lower FA (F), higher MD (G), RD (H), and AD (I), compared with MS-TN patients (solid blue, n = 15). **P* < 0.05, ***P* < 0.01 (FDR-corrected). CN V = trigeminal nerve. AD, axial diffusivity; DTI, diffusion tensor imaging; FA, fractional anisotropy; FDR, false discovery rate; MD, mean diffusivity; MS, multiple sclerosis; RD, radial diffusivity; ROI, region of interest; TN, trigeminal neuralgia.

Trigeminal neuralgia associated with brainstem lesions is considered rare and has not been defined as its own syndrome. To the best of our knowledge, only a total of 13 cases of TN patients with brainstem lesions have been previously reported.^{3,6,23,24,34,38} Chang et al.⁶ reported 2 cases treated with Gamma Knife radiosurgery, including one patient with bilateral TN and bilateral pontine lesions. They suggested an old pontine viral neuritis as a possible cause of the lesion for both patients. Arrese et al.³ reported 4 cases and suggested demyelination or ischemia as the likely nature of the lesion. Although Neetu et al.³⁴ also reported 4 similar cases and used DTI to identify microstructural abnormalities, they examined the trigeminal root entry zone and not the brainstem lesion of these patients. There are also 3 single case reports of TN resulting from pontine infarction.^{23,24,38} In this study, we identify 24 cases of SPL-TN out of our pool of 481 TN patients. Thus, based on our cohort, approximately 1 in 20 patients with TN have a pontine lesion. This suggests that this syndrome may be far more common amongst people with TN than previously believed.

There are several limitations to this study. Given the long-standing history of TN and refractory nature of the SPL-TN cohort, we were unable to limit our study to patients with surgically naïve imaging. To ensure that the lesion is not an effect of surgery, we demonstrated that there is no significant change in T1 lesion volume and location in a subset of patients who had imaging before and after treatment. Furthermore,

none of the patients reported significant sensory changes as a result of surgery, including paresthesia or numbness—one would expect this if the lesion was a surgical complication. Nonetheless, our lesion mapping and DTI findings may have been influenced by previous surgery. A prospective corroborative study on surgically naïve patients may be merited. Another limitation is the retrospective nature of the study. However, this approach led to the discovery of this unusual clinical group and comprehensive examination of their clinical and neuroimaging characteristics. Thus, this retrospective study serves as an important foundation for defining this syndrome and future prospective studies are merited to gain further insight. Our sample size was also relatively small. However, this is the largest and most comprehensive study to date that provides a clear definition of this entity as its own syndrome. Overall, we highlight the importance of future research across multiple domains (eg, neuroimaging, neurophysiology, and histology) to further understand this unique clinical syndrome and its potential etiology.

In conclusion, our study defines a new clinical syndrome of SPL-TN. Advanced neuroimaging techniques reveal the centralized location of these lesions and pinpoints their microstructural differences from MS plaques. Given the refractory nature of this syndrome, identifying SPL-TN as a distinct subset may be important in the clinical setting as it will guide treatment decision-making.

Conflict of interest statement

The authors have no conflicts of interest to declare.

Acknowledgements

The authors thank Powell Chu for expert technical assistance. This work was supported by the Canadian Institutes of Health Research (operating grant to MH, Ref. # MOP130555). S. Tohyama and P. Hung are recipients of the Canadian Institutes of Health Research Doctoral Research Award (Ref. # GSD164127 and GSD157876).

Article history:

Received 6 September 2019

Received in revised form 29 November 2019

Accepted 6 December 2019

Available online 9 December 2019

References

- Alexander AL, Lee JE, Lazar M, Field AS. Diffusion tensor imaging of the brain. *Neurotherapeutics* 2007;4:316–29.
- Antonini G, Di Pasquale A, Cruccu G, Truini A, Morino S, Saltelli G, Romano A, Trasimeni G, Vanacore N, Bozzao A. Magnetic resonance imaging contribution for diagnosing symptomatic neurovascular contact in classical trigeminal neuralgia: a blinded case-control study and meta-analysis. *PAIN* 2014;155:1464–71.
- Arese I, Lagares A, Alday R, Ramos A, Rivas JJ, Lobato RD. Typical trigeminal neuralgia associated with brainstem white matter lesions on MRI in patients without criteria of multiple sclerosis. *Acta Neurochir* 2008;150:1157–61.
- Avants BB, Tustison NJ, Song G, Cook PA, Klein A, Gee JC. A reproducible evaluation of ANTs similarity metric performance in brain image registration. *Neuroimage* 2011;54:2033–44.
- Bakker NA, Van Dijk JM, Immenga S, Wagemakers M, Metzemaekers JD. Repeat microvascular decompression for recurrent idiopathic trigeminal neuralgia. *J Neurosurg* 2014;121:936–9.
- Chang JW, Choi JY, Yoon YS, Park YG, Chung SS. Unusual causes of trigeminal neuralgia treated by gamma knife radiosurgery: report of two cases. *J Neurosurg* 2002;97:533–5.
- Chen DQ, DeSouza DD, Hayes DJ, Davis KD, O'Connor P, Hodaie M. Diffusivity signatures characterize trigeminal neuralgia associated with multiple sclerosis. *Mult Scler* 2016;22:51–63.
- DeSouza DD, Hodaie M, Davis KD. Abnormal trigeminal nerve microstructure and brain white matter in idiopathic trigeminal neuralgia. *PAIN* 2014;155:37–44.
- DeSouza DD, Davis KD, Hodaie M. Reversal of insular and microstructural nerve abnormalities following effective surgical treatment for trigeminal neuralgia. *PAIN* 2015;156:1112–23.
- Devor M, Govrin-Lippmann R, Rappaport ZH. Mechanism of trigeminal neuralgia: an ultrastructural analysis of trigeminal root specimens obtained during microvascular decompression surgery. *J Neurosurg* 2002;96:532–43.
- Dhople AA, Adams JR, Maggio WW, Naqvi SA, Regine WF, Kwok Y. Long-term outcomes of gamma knife radiosurgery for classic trigeminal neuralgia: implications of treatment and critical review of the literature: clinical article. *J Neurosurg* 2009;111:351–8.
- Di Stefano G, Maarbjerg S, Truini A. Trigeminal neuralgia secondary to multiple sclerosis: from the clinical picture to the treatment options. *J Headache Pain* 2019;20:20.
- Eller JL, Raslan AM, Burchiel KJ. Trigeminal neuralgia: definition and classification. *Neurosurg Focus* 2005;18:E3.
- Fedorov A, Beichel R, Kalpathy-Cramer J, Finet J, Fillion-Robin JC, Pujol S, Bauer C, Jennings D, Fennessy F, Sonka M, Buatti J, Aylward S, Miller JV, Pieper S, Kikinis R. 3D slicer as an image computing platform for the quantitative imaging network. *Magn Reson Imaging* 2012;30:1323–41.
- Frohman EM, Racke MK, Raine CS. Multiple sclerosis—the plaque and its pathogenesis. *N Engl J Med* 2006;354:942–55.
- Fromm GH, Terrence CF, Maroon JC. Trigeminal neuralgia. Current concepts regarding etiology and pathogenesis. *Arch Neurol* 1984;41:1204–7.
- Harries AM, Mitchell RD. Percutaneous glycerol rhizotomy for trigeminal neuralgia: safety and efficacy of repeat procedures. *Br J Neurosurg* 2011;125:268–72.
- Headache Classification Committee of the International Headache Society (IHS). The International Classification of Headache Disorders, 3rd edition. *Cephalalgia* 2018;38:1–211.
- Herweh C, Kress B, Rasche D, Tronnier V, Troger J, Sartor K, Stippich C. Loss of anisotropy in trigeminal neuralgia revealed by diffusion tensor imaging. *Neurology* 2007;68:776–8.
- Hodaie M, Coello AF. Advances in the management of trigeminal neuralgia. *J Neurosurg Sci* 2013;57:13–21.
- Hung PS, Chen DQ, Davis KD, Zhong J, Hodaie M. Predicting pain relief: use of pre-surgical trigeminal nerve diffusion metrics in trigeminal neuralgia. *Neuroimage Clin* 2017;15:710–18.
- Jenkinson M, Beckmann CF, Behrens TE, Woolrich MW, Smith SM. FSL. *Neuroimage* 2012;62:782–90.
- Katsuno M, Teramoto A. Secondary trigeminal neuropathy and neuralgia resulting from pontine infarction. *J Stroke Cerebrovasc Dis* 2010;19:251–2.
- Kim JS, Kang JH, Lee MC. Trigeminal neuralgia after pontine infarction. *Neurology* 1998;51:1511–12.
- Kondziolka D, Zorro O, Lobato-Polo J, Kano H, Flannery TJ, Flickinger JC, Lunsford LD. Gamma Knife stereotactic radiosurgery for idiopathic trigeminal neuralgia. *J Neurosurg* 2010;112:758–65.
- Koopman JS, Dieleman JP, Huygen FJ, de Mos M, Martin CG, Sturkenboom MC. Incidence of facial pain in the general population. *PAIN* 2009;147:122–7.
- Kugelberg E, Lindblom U. The mechanism of the pain in trigeminal neuralgia. *J Neurol Neurosurg Psychiatry* 1959;22:36–43.
- Leal PR, Roch JA, Hermier M, Souza MA, Cristino-Filho G, Sindou M. Structural abnormalities of the trigeminal root revealed by diffusion tensor imaging in patients with trigeminal neuralgia caused by neurovascular compression: a prospective, double-blind, controlled study. *PAIN* 2011;152:2357–64.
- Liu GT. The trigeminal nerve and its central connections. In: Miller NR, Walsh FB, Hoyt WF, editors. *Walsh and Hoyt's clinical neuro-ophthalmology*. Philadelphia: Lippincott Williams & Wilkins, 2005. p. 1233–74.
- Love S, Coakham HB. Trigeminal neuralgia: pathology and pathogenesis. *Brain* 2001;124:2347–60.
- Lutz J, Linn J, Mehrkens JH, Thon N, Stahl R, Seelos K, Bruckmann H, Holtmannspotter M. Trigeminal neuralgia due to neurovascular compression: high-spatial-resolution diffusion-tensor imaging reveals microstructural neural changes. *Radiology* 2011;258:524–30.
- Maarbjerg S, Wolfram F, Gozalov A, Olesen J, Bendtsen L. Significance of neurovascular contact in classical trigeminal neuralgia. *Brain* 2015;138:311–19.
- Meaney JF, Watt JW, Eldridge PR, Whitehouse GH, Wells JC, Miles JB. Association between trigeminal neuralgia and multiple sclerosis: role of magnetic resonance imaging. *J Neurol Neurosurg Psychiatry* 1995;59:253–9.
- Neetu S, Sunil K, Ashish A, Jayantee K, Usha Kant M. Microstructural abnormalities of the trigeminal nerve by diffusion-tensor imaging in trigeminal neuralgia without neurovascular compression. *Neuroradiol J* 2016;29:13–18.
- Nurmikko TJ, Eldridge PR. Trigeminal neuralgia—pathophysiology, diagnosis and current treatment. *Br J Anaesth* 2001;87:117–32.
- Oesman C, Mooij JJ. Long-term follow-up of microvascular decompression for trigeminal neuralgia. *Skull Base* 2011;21:313–22.
- Park KJ, Kondziolka D, Berkowitz O, Kano H, Novotny J Jr, Niranjan A, Flickinger JC, Lunsford LD. Repeat gamma knife radiosurgery for trigeminal neuralgia. *Neurosurg* 2012;70:295–305; discussion 305.
- Peker S, Akansel G, Sun I, Pamir NM. Trigeminal neuralgia due to pontine infarction. *Headache* 2004;44:1043–5.
- Popescu BF, Lucchinetti CF. Pathology of demyelinating diseases. *Annu Rev Pathol* 2012;7:185–217.
- Qazi AA, Radmanesh A, O'donnell L, Kindlmann G, Peled S, Whalen S, Westin CF, Golby AJ. Resolving crossings in the corticospinal tract by two-tensor streamline tractography: method and clinical assessment using fMRI. *Neuroimage* 2009;47:T98–T106.
- Regis J, Tuleasca C, Resseguier N, Carron R, Donnet A, Gaudart J, Levivier M. Long-term safety and efficacy of Gamma Knife surgery in classical trigeminal neuralgia: a 497-patient historical cohort study. *J Neurosurg* 2016;124:1079–87.
- Song SK, Sun SW, Ramsbottom MJ, Chang C, Russell J, Cross AH. Dysmyelination revealed through MRI as increased radial (but unchanged axial) diffusion of water. *Neuroimage* 2002;17:1429–36.
- Song SK, Sun SW, Ju WK, Lin SJ, Cross AH, Neufeld AH. Diffusion tensor imaging detects and differentiates axon and myelin degeneration in mouse optic nerve after retinal ischemia. *Neuroimage* 2003;20:1714–22.
- Song SK, Yoshino J, Le TQ, Lin SJ, Sun SW, Cross AH, Armstrong RC. Demyelination increases radial diffusivity in corpus callosum of mouse brain. *Neuroimage* 2005;26:132–40.

- [45] Thompson AJ, Banwell BL, Barkhof F, Carroll WM, Coetzee T, Comi G, Correale J, Fazekas F, Filippi M, Freedman MS, Fujihara K, Galetta SL, Hartung HP, Kappos L, Lublin FD, Marrie RA, Miller AE, Miller DH, Montalban X, Mowry EM, Sorensen PS, Tintore M, Traboulsee AL, Trojano M, Uitdehaag BMJ, Vukusic S, Waubant E, Weinshenker BG, Reingold SC, Cohen JA. Diagnosis of multiple sclerosis: 2017 revisions of the McDonald criteria. *Lancet Neurol* 2018;17:162–73.
- [46] Tohyama S, Shih-Ping Hung P, Zhong J, Hodaie M. Early postsurgical diffusivity metrics for prognostication of long-term pain relief after Gamma Knife radiosurgery for trigeminal neuralgia. *J Neurosurg* 2018;131:539–48.
- [47] Tolle T, Dukes E, Sadosky A. Patient burden of trigeminal neuralgia: results from a cross-sectional survey of health state impairment and treatment patterns in six European countries. *PAIN Pract* 2006;6:153–60.
- [48] Williams CG, Dellon AL, Rosson GD. Management of chronic facial pain. *Craniomaxillofac Trauma Reconstr* 2009;2:67–76.
- [49] Xia L, Zhong J, Zhu J, Wang YN, Dou NN, Liu MX, Visocchi M, Li ST. Effectiveness and safety of microvascular decompression surgery for treatment of trigeminal neuralgia: a systematic review. *J Craniofac Surg* 2014;25:1413–17.
- [50] Xu Z, Mathieu D, Heroux F, Abbassy M, Barnett G, Mohammadi AM, Kano H, Caruso J, Shih HH, Grills IS, Lee K, Krishnan S, Kaufmann AM, Lee JYK, Alonso-Basanta M, Kerr M, Pierce J, Kondziolka D, Hess JA, Gerrard J, Chiang V, Lunsford LD, Sheehan JP. Stereotactic radiosurgery for trigeminal neuralgia in patients with multiple sclerosis: a multicenter study. *Neurosurgery* 2019;84:499–505.
- [51] Zorro O, Lobato-Polo J, Kano H, Flickinger JC, Lunsford LD, Kondziolka D. Gamma knife radiosurgery for multiple sclerosis-related trigeminal neuralgia. *Neurology* 2009;73:1149–54.